IEEE Access
Multidisciplinary | Rapid Review | Open Access Journal

Received May 9, 2019, accepted May 29, 2019, date of publication June 5, 2019, date of current version June 21, 2019.

Digital Object Identifier 10.1109/ACCESS.2019.2920839

Design of Wideband Circularly Polarized Crossed-Dipole Antenna Using Parasitic Modified Patches

ZHIPENG ZHAO, YAPENG LI, MENG XUE, LE WANG, ZHAOYANG TANG, AND YINGZENG YIN

National Key Laboratory of Antennas and Microwave Technology, Xidian University, Xi'an, Shaanxi 710071, China

Corresponding author: Yingzeng Yin (yyzeng@mail.xidian.edu.cn)

ABSTRACT In this paper, a wideband circularly polarized (CP) crossed-dipole antenna is presented by using parasitic modified patches. Four polygonal metal patches are sequentially rotated around the crossed dipoles. By tuning the electromagnetic coupling characteristic between the patches and the crossed dipoles, the axial-ratio bandwidth (ARBW) of the lower frequency band can be enhanced significantly. Furthermore, four slots are etched on the parasitic patches in a sequential rotation way, modifying the current distribution. Therefore, an extra CP mode produces at the higher band. A wide 3-dB ARBW is realized by combing three CP modes, including the basic CP mode of the cross dipole at the middle frequency band. A prototype of the proposed broadband CP antenna was manufactured and measured to verify the design principle. The measurement results illustrate that the antenna has a wide 10-dB return loss bandwidth of 99.2% (1.24–3.68 GHz) and a broad 3-dB ARBW of 72.7% (1.41–3.02 GHz) for right-hand circular polarization (RHCP). Besides, stable gain and unidirectional radiation patterns are also obtained over the entire band of operation.

INDEX TERMS Circularly polarized (CP), crossed-dipole, electromagnetic coupling characteristic, parasitic modified patches, wideband.

I. INTRODUCTION

In recent years, circularly polarized antennas have attracted more and more attention due to their low multipath interference and excellent polarization matching performance. With the multifunctional development of wireless communication devices, the demand for antennas with outstanding performance such as broadband, miniaturization and high gain is increased.

Various types of broadband CP antennas have been developed by researchers. The low-profile patch antenna with a parasitic patch and vertical metallic plates [1] obtains a good ARBW. Dielectric resonator antennas can be utilized to realize the CP performance of wideband and high efficiency [2], [3]. Besides, it is also an excellent method to obtain a wide CP work band by designing a wideband feeding network [4]–[6]. Combining three Wilkinson power dividers, two wideband 90° phase shifters and a wideband 180° phase shifter [4], the antenna obtains an impedance bandwidth (IBW) of 65% and an ARBW of 75%. The proposed feeding network with identical amplitude and flat 90° shifts in [5] helps the antenna get an excellent ARBW. The wide slot antennas offer a broad IBW and ARBW with microstrip fed [7], [8] as well as CPW fed [9], [10]. The presented slot antenna in [8] has a measured IBW of 124.4% and a 3-dB ARBW of 115.2%.

To obtain the performances of wideband, high gain and good unidirectional radiation, crossed dipoles are generally used. Two orthogonal liner dipoles connected by two 90° phase delay lines are proposed in [11] to obtain an ARBW of 15.6%. The phase delay line owns a simpler structure but a narrow bandwidth. With the dual back cavity, the ARBW can be extended to 66.7% [12]. Crossed dipoles with wide open ends [13] as well as parasitic loops [14] are also good candidates to improve ARBW.

To further increase the ARBW, some other design methodologies are studied. The asymmetric crossed bowtie dipoles with a back cavity [15] achieve a wide ARBW of 51%. The crossed dipoles encircled by an asymmetrical loop in [16] also obtain an excellent ARBW of 53.4%. A single bowtie-shaped parasitic element and a back cavity are employed to realize an ARBW of 58.6% [17]. The ARBWs of the above cross-dipole antennas are not wide enough. The antenna proposed in [18] is successful in enhancing the ARBW to 106.1%

The associate editor coordinating the review of this manuscript and approving it for publication was Yang Yang.

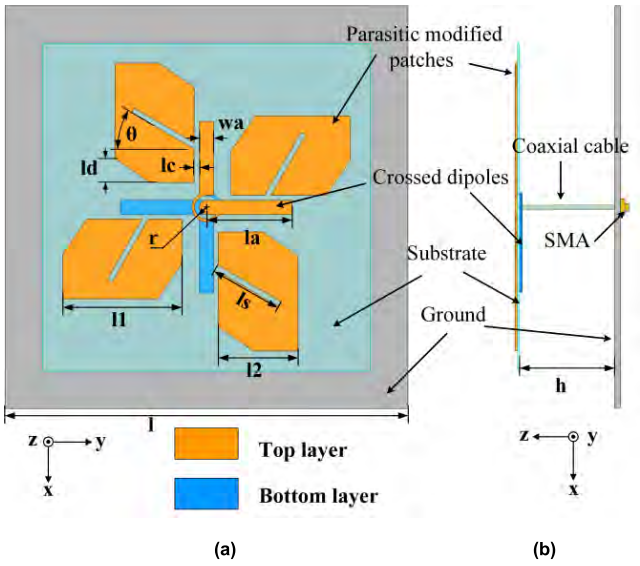

FIGURE 1. Configuration of the proposed antenna: (a) Top view and (b) Side view.

with four metallic plates vertically added on the ground. Complex back cavities are introduced to improve the ARBWs in [19] and [20]. Another broadband CP antenna presented in [21] consists of a crossed bowtie dipole, four unequal parasitic crossed slots, four parasitic bowtie patches and four parasitic rectangular strips. A recent work in [22] with two kinds of parasitic elements also obtains a good performance. Although there are a large number of broadband crossed-dipole antennas, they are still not excellent enough to meet various communication requirements.

In this paper, a broadband circularly polarized antenna with parasitic modified patches is presented. On the one hand, four polygonal metal patches are employed to widen the lower operational bandwidth. On the other hand, different from the previous works, four slots sequentially etched on the patches are utilized to expand the higher working bandwidth. Hence, the proposed CP antenna owns an excellent CP performance. Measured results show that the proposed antenna obtains a broad 10-dB IBW of 99.2%, a wide 3-dB ARBW of 72.7% and a peak gain of 10 dBi.

II. ANTENNA DESIGN AND ANALYSIS

A. ANTENNA GEOMETRY

The configuration of the proposed CP antenna is displayed in Fig.1. The substrate in this design is F4BM-2 with a thickness of 0.8 mm, a relative permittivity of 2.65, and a loss tangent of 0.002. The two crossed dipoles are connected by two 90° phase delay rings and printed on both layers of the substrate. Four parasitic modified patches are sequentially rotated around the crossed dipoles and etched on the top layer of the substrate. Each liner slot has a specific angle to the axis. A metal ground plane is placed below the antenna with a distance of 37.5mm to obtain a unidirectional radiation. The antenna is fed by a 50-Ω coaxial cable, of which the inner conductor is connected to the arms of the crossed dipoles

TABLE 1. Dimensions of the antenna (unit: mm).

l	h	θ	l1	l2	la	wa	ls	lc	ld	r
150	37.5	30°	43.3	29.5	31.9	5.2	27	1.9	9	4.4

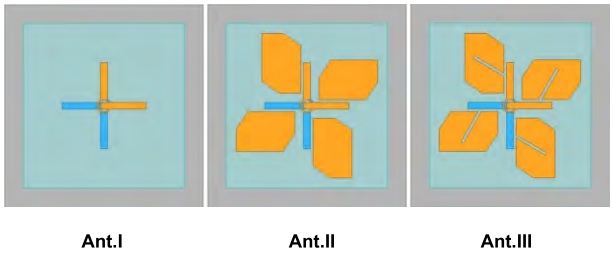

FIGURE 2. Evolution of the proposed antenna.

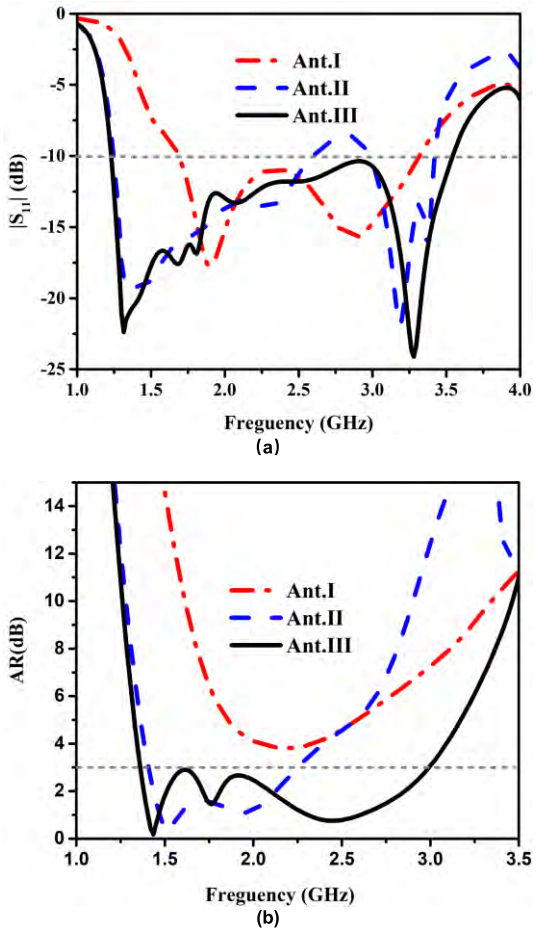

FIGURE 3. Performance comparison between different antennas: (a) $|S_{11}|$, (b) AR.

on the top side of the substrate and the outer conductor soldered to the ground plane and the arms on the bottom side. This project is built and simulated in HFSS v. 18, and Table 1 exhibits the optimized dimensions of the geometry.

B. EVOLUTION OF THE CP ANTENNA

Fig.2 illustrates the evolution of the proposed antenna. Ant. I is a pair of crossed dipoles connected with 90° phase delay lines. It can be seen from Fig.3 that Ant. I exhibits a narrow

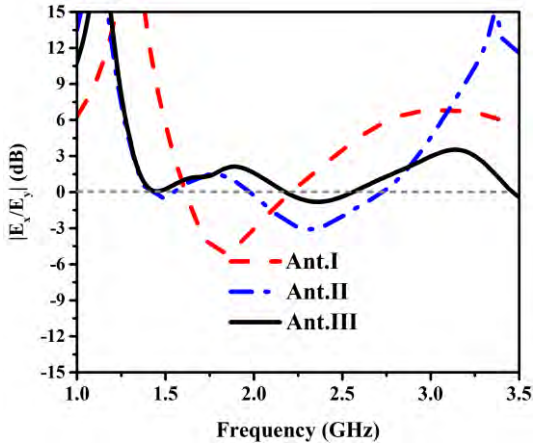

(a)

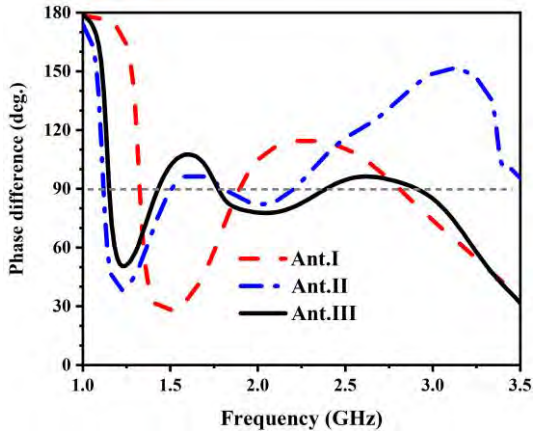

(b)

FIGURE 4. **(a) Amplitude ratio($|E_x/E_y|$) and (b) Phase difference.**

impedance band with bad ARBW. With four polygonal metal patches added, Ant. II is extended both in IBW and ARBW. An additional CP mode can be observed at the lower band, which contributes to a better ARBW. By etching four sequentially rotational slots at the edges of the patches (Ant. III), an extra CP mode generates in the higher band. And the ARBW has been dramatically improved from 46.57% (Ant. II) to74.9%.

In order to generate CP waves, we need to implement two orthogonal electric fields with a phase difference of 90°. Fig.4 shows the amplitude ratio and the phase difference between the electric field in the x-axis (**Ex**) and y-axis (**Ey**) directions. In Ant. I, the ARBW is primarily determined by the two 90° phase delay rings, which provides a single CP mode with a narrow band. With four polygonal metal patches added in Ant. II, the amplitude ratio of **Ex** to **Ey** at about 1.4 GHz is significantly improved. When the phase difference is close to 90°, Ant. II generates an extra CP mode. By adjusting the size and position of the patches, CP waves can be easily realized at the lower band. However, it can be observed in Fig.4 (b) that Ant. II has a poor phase difference at 2.75GHz. To solve this problem, the parasitic modified patches (Ant. III) are used. By adjusting the length and angle

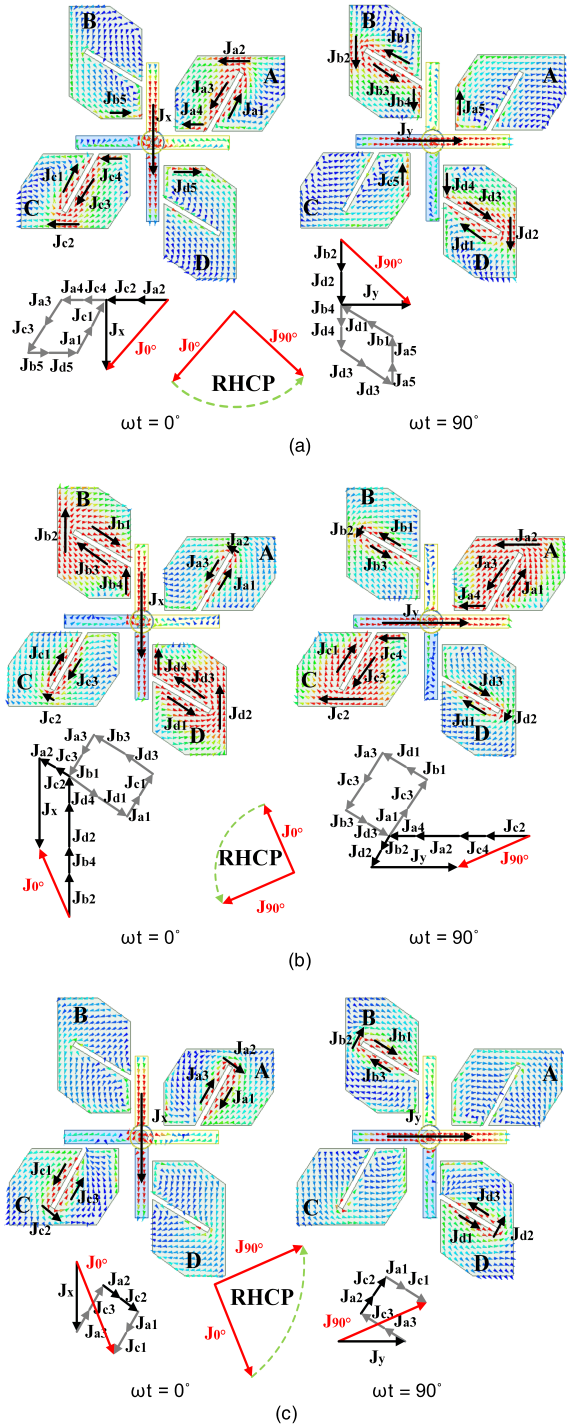

FIGURE 5. **Current distributions of the proposed antenna: (a) f = 1.4 GHz, (b) f = 1.75 GHz, and (c) f = 2.5GHz.**

of the slots on the parasitic modified patches, the phase difference at the higher band is tuned to around 90°. Thus, another CP mode produces.

C. ANALYSIS OF SURFACE CURRENT DISTRIBUTION

To further investigate the working mechanism of the three CP modes, current distributions on the antenna at three resonance frequencies for different angular times are plotted in Fig.5.

The surface current on Patch A and C is mainly excited by the horizontal dipoles. Similarly, the surface current on Patch B and D is mainly excited by the vertical dipoles.

As can be seen in Fig. 5(a), when $\omega t = 0°$ at 1.4 GHz, the dominant currents consist of **Jx** on crossed dipoles, **Ja1**, **Ja2**, **Ja3**, **Ja4**, **Jb5**,**Jc1**, **Jc2**, **Jc3**, **Jc4,** and **Jd5** on the parasitic modified patches. It is noteworthy that part of the surface currents on the parasitic modified patches cancels each other out and the surface current on the horizontal dipole is weak which leads to electric coupling. As a result, the superimposed current for 0° phase depends on **Jx**, **Ja2** and **Jc2**. **Ja2** and **Jc2** on parasitic modified patches are in the y-axis direction while **Jx** on crossed dipoles is towards the x-axis direction. When $\omega t = 90°$ at 1.4GHz, the dominant currents consist of **Jy** on crossed dipoles, **Ja5**, **Jb1**, **Jb2**, **Jb3**, **Jb4**, **Jc5**, **Jd1**, **Jd2**, **Jd3** and **Jd4** on the parasitic modified patches. The superimposed current of the antenna has a rotation of 90° counterclockwise, thereby generating RHCP.

When $\omega t = 0°$ at 1.75 GHz in Fig. 5(b), a mainly magnetic coupling is generated as the surface current on the vertical dipole reaches its maximum value. **Ja3** and **Jc3** cancel out with **Ja1** and **Jc1**. **Ja2** and **Jc2** are so weak that they can be ignored. So the direction is mainly biased toward the - y-axis which is opposite to the surface current **Jx**. The superimposed current for 0° phase depends on **Ja2**, **Jb2**, **Jc2**, **Jd2**, **Jb4** and **Jd4**. When $\omega t = 90°$ at 1.75GHz, the superimposed current has a rotation of 90° counterclockwise which is the same as the case at 1.4 GHz. In this time, the CP mode is mainly generated by the crossed dipoles, and the magnetic coupled parasitic modified patches enhance the CP resonance mode.

When the proposed antenna works at 2.5 GHz in Fig. 5(c), the electric coupled surface currents on the parasitic modified patches mainly distribute around the slots. It means that the slots and the crossed dipoles are the primary radiators not the outer edge of the parasitic modified patches. Compared to Ant. II, four slots composing a pair of crossed-slot antennas rotate around the crossed dipoles to produce an additional CP mode. **Ja1** and **Jc1** cancel out with **Ja3** and **Jc3**. **Jb1** and **Jd1** cancel out with **Jb3** and **Jd3**. So the superimposed current is mainly controlled by **Jx**, **Jy**, **Ja2**, **Jb2**, **Jc2** and **Jd2** which produces CP waves.

D. PARAMETERS STUDIES

A parametric study on AR is investigated in this subsection. To better understand the effect of parameter changes on AR, the amplitude ratio and the phase difference between the electric field in the x-axis (**Ex**) and y-axis (**Ey**) directions are also plotted. As one design parameter is studied at a time, the others remain the optimized values listed in Table 1.

The effect of the gap lc between the parasitic modified patches and the crossed dipoles on AR is plotted in Fig.6. When reducing the gap lc, a left shift of three CP modes can be observed. This is due to the fact that the larger

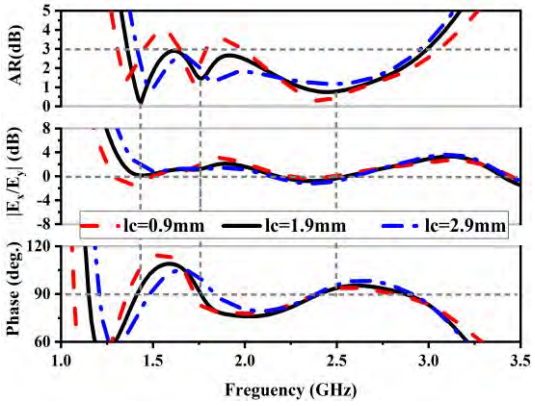

FIGURE 6. Effect of different values of lc on AR, the amplitude ratio and the phase difference.

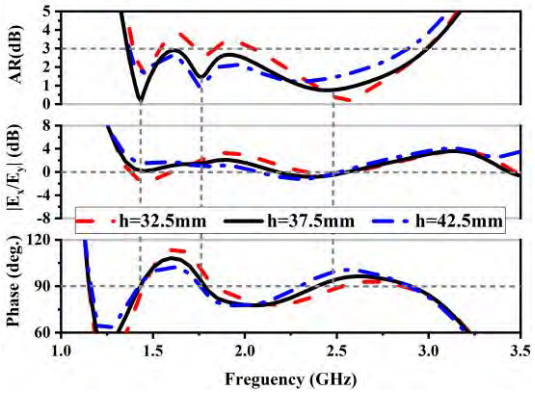

FIGURE 7. Effect of different values of h on AR, the amplitude ratio and the phase difference.

coupling capacitance makes the curve shift to the low frequency. Reducing the gap lc will also improve the phase difference of the lower mode and the amplitude ratio of the middle mode, but the operation band will be narrow. On the other hand, the influence of the height h from the ground plane to the radiation patch on improving the ARBW is evaluated in Fig.7. When varying the parameter h, another shift of three CP modes can be observed. Increasing the height h will improve the amplitude ratio and the phase difference at the lower- and middle-frequency bands, making the ARBW better. But the amplitude ratio at the higher band will be worse, making the operation narrow. Therefore, a trade-off is made between ls and h to avoid damaging the lower and middle band and obtain a wide ARBW. Besides, it is necessary to be taken into consideration that a large h will destroy the radiation patterns. Finally, lc = 1.9 mm and h = 37.5 mm are chosen for obtaining a wide ARBW.

The optimal length ls of the slots and angle θ are also investigated. A left shift of the ARBW can be observed from Fig.8 when the value of ls increases. It can be got from Fig.5 that an increase of the length ls means an extension of the surface current path. Besides, the curve goes down at around 2 GHz because of the phase difference being

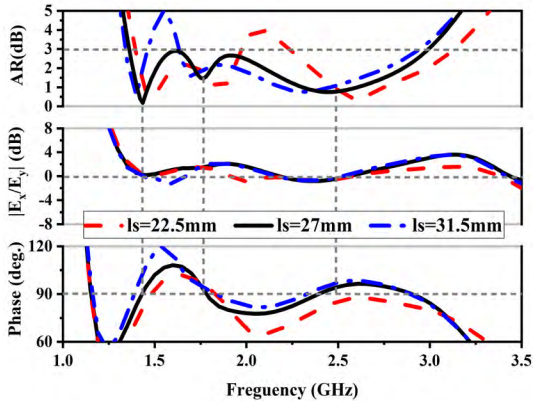

FIGURE 8. Effect of different values of ls on AR, the amplitude ratio and the phase difference.

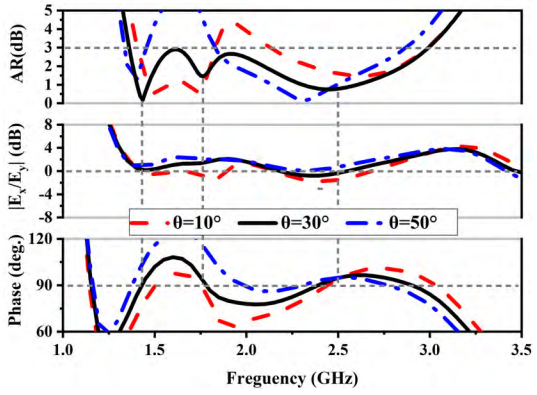

FIGURE 9. Effect of different values of θ on AR, the amplitude ratio and the phase difference.

improved but goes up at around 1.6 GHz because of the phase difference getting worse. On the other hand, when the slots rotate from 10° to 30°, the first and third CP modes move toward the lower frequency band in Fig.9 because of the left shift of the phase difference. The performance of CP is much improved at around 2 GHz as a good phase difference is obtained. However, the ARBW significantly deteriorates at around 1.6 GHz when θ is 50° since the phase difference gets worse. At the same time, a down shift of the higher CP resonance mode can be observed because of a better phase difference. So, suitable values of the parameters ls and θ are chosen to gain a desirable broad ARBW.

As can be seen from Fig.10, the size ld of the chamfers on the parasitic modified patches has an obvious impact on the middle and higher ARBWs. The second and third CP resonance modes move to the higher frequency band when ld increases. It is because the curve of the phase difference has a right shift at the middle and higher bands. But the first CP resonance mode almost remains almost unchanged. As ld gets larger than 9 mm, the curve of the middle band moves upward, and the AR appears deteriorative points at around 1.7GHz due to the deterioration of the amplitude ratio and the phase difference. Hence, a proper size of chamfers is absolutely essential to obtain a broad ARBW.

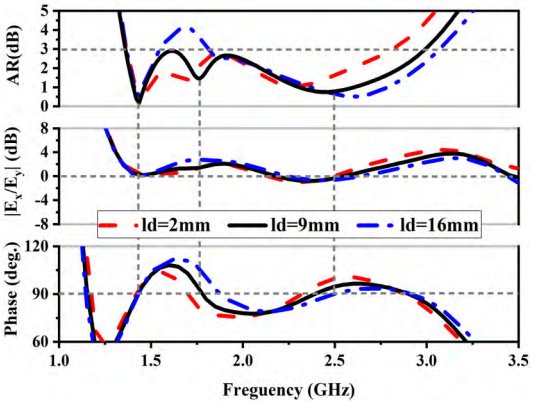

FIGURE 10. Effect of different values of ld on AR, the amplitude ratio and the phase difference.

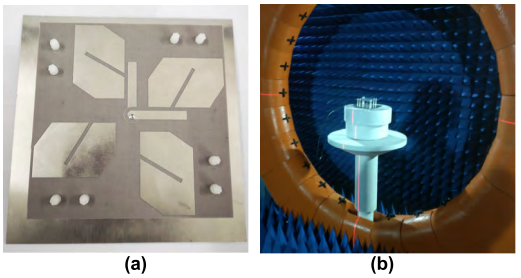

FIGURE 11. Photographs of the fabricated antenna (a) and testing the antenna in microwave anechoic chamber (b).

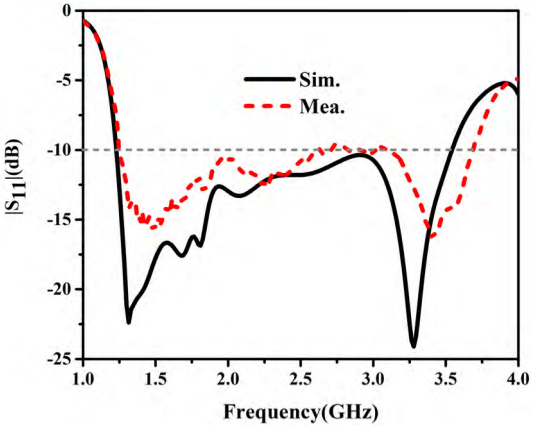

FIGURE 12. Simulated and measured $|S_{11}|$ of the proposed antenna.

III. EXPERIMENTAL RESULTS

For validation, the proposed broadband CP antenna was fabricated and measured as showed in Fig. 11. Fig. 12 plots the simulated and measured reflection coefficients of the CP antenna. The measured −10 dB IBW is 99.2% (1.24-3.68 GHz), agreeing well with the simulated result (1.22-3.53 GHz). The measured and simulated axial ratio bandwidths and gains are plotted in Fig. 13. It can be observed that the measured 3-dB ARBW is 72.7% (1.41-3.02 GHz) while the simulated ARBW is 74.9% (1.36-2.99 GHz). The measured curves have a slight shift to the right which can be accepted because of the fabrication tolerance.

TABLE 2. Performance compariso.

Ref.	Size (λ_0^3)	IBW	ARBW	Over	Peak Gain	Techniques
[12]	0.86×0.86×0.36	79.4%(1.9-4.4 G)	66.7%(2-4 GHz)	66.7%		A dual-cavity structure
[15]	1.0×1.0×0.26	57%(1.77-3.19 GHz)	51%(2.05-3.45 GHz)	43.5%	9.6 dBi	Asymmetric bowtie dipoles
[16]	1.1×1.1×0.28	67.5%(3.14-6.32 GHz)	53.4%(3.83-6.62 GHz)	49.4%	10.6 dBi	A single parasitic cross-loop
[17]	0.79×0.79×0.27	68.9%(1.9-3.9 GHz)	58.6%(2.05-3.75 GHz)	58.6%	9.4 dBi	A simple single parasitic element
[18]	0.59×0.59×0.24	115.2%(0.84-3.12 GHz)	106.1%(0.92-3 GHz)	106.1%	6.7 dBi	Vertical metallic plates
[19]	π×0.84×0.84×0.35	106.5%(0.9-2.95 GHz)	96.6%(1-2.87 GHz)	96.6%		Elliptical dipoles with a composite cavity
[20]	π×0.42×0.42×0.35	107%(0.96-3.12 GHz)	97%(1.08-3.12GHz)	97%	< 10 dBi	Parasitic arrow-shaped patches with a inverted cylindrical cavity
[22]	0.92×0.92×0.225	77.6%(1.11-2.52 GHz)	66%(1.25-2.48GHz)	66%	8.4 dBi	two kinds of parasitic elements
Pro.	1.11×1.11×0.28	99.2%(1.24-3.68 GHz)	72.7%(1.41-3.02 GHz)	72.7%	10.1 dBi	Parasitic modified patches

Here λ_0 is the wavelength at CP center frequency

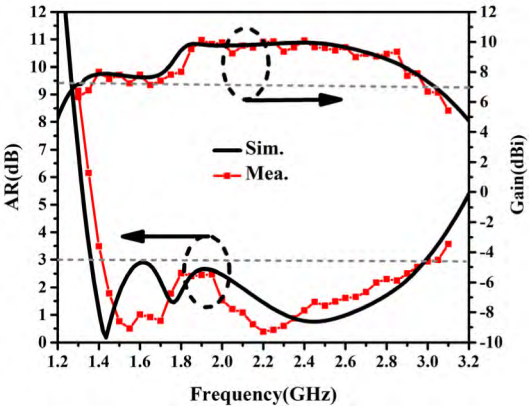

FIGURE 13. Simulated and measured AR and gain of the proposed antenna.

The measured gain varies from 6.68 dBi to 10.12 dBi within the operation band and a 3-dB gain bandwidth of 71.5% (1.41-2.98GHz) is obtained in boresight. The simulated and measured radiation patterns at 1.75 GHz, 2.5 GHz and 3 GHz show good agreements, as depicted in Fig. 14. The measured 3-dB beamwidths are 60° and 56° at 1.75GHz, 59° and 62° at 2.5GHz, 58° and 93° at 3GHz in xoz-plane and yoz-plane, respectively. The proposed antenna achieves stable and unidirectional radiation patterns with low back lobes as well as low cross-polarizations across the whole operation band since it has a larger ground plane, and lower profile.

Table 2 lists the comparison of performance between the proposed and the reported CP crossed-dipole antennas. Obviously, the proposed antenna has a wider overlapping bandwidth than the antennas in [12], [15]–[17], and [22], and a lower profile than the ones in [12] [19], and [20]. With almost the same aperture efficiency, the proposed antenna has a larger gain than the design in [18] and a more stable gain than the work in [19]. Although the crossed dipoles in [18]–[20] have wider ARBW, the proposed antenna has lower cost and a simpler structure for fabrication. Besides, the antenna has an outstanding 3-dB gain bandwidth as well as stable radiation patterns.

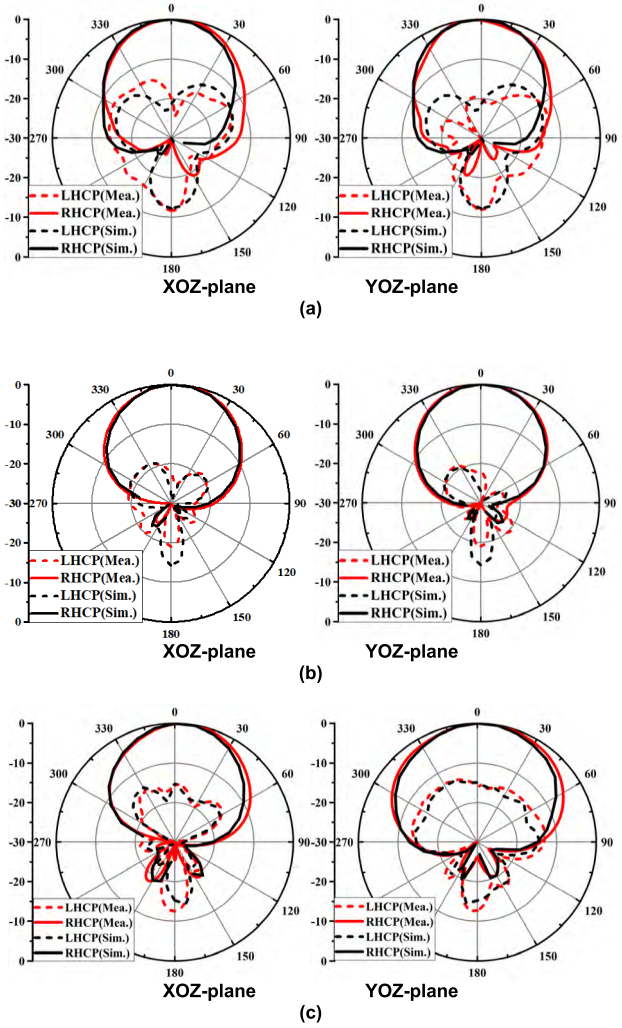

FIGURE 14. Simulated and measured radiation patterns at (a) 1.75GHz, (b) 2.5GHz, (c) 3GHz.

IV. CONCLUSION

A wideband circularly polarized antenna with parasitic modified patches is investigated in this paper. By introducing four polygonal metal patches distributed around the crossed

dipoles, the ARBW is greatly improved at the lower frequency band. Moreover, four slots sequentially etched on the parasitic elements are added to produce a new CP mode at the higher frequency band. Thus, a wide ARBW is obtained. The proposed antenna is fabricated, measured and analyzed. The measured results show that the proposed CP antenna has an excellent impedance bandwidth of 99.2% from 1.24 to 3.68 GHz, and a 3-dB ARBW of 72.7% from 1.41 to 3.02 GHz. Stable radiation gain and unidirectional radiation patterns are also realized. The proposed broadband circularly polarized antenna will be an excellent candidate for wireless communication application.

REFERENCES

[1] J. Li, H. Liu, S. Zhang, M. Luo, Y. Zhang, and S. He, "A wideband single-fed, circularly-polarized patch antenna with enhanced axial ratio bandwidth for UHF RFID reader applications," *IEEE Access*, vol. 6, pp. 55883–55892, Oct. 2018.

[2] R. Chowdhury, N. Mishra, M. M. Sani, and R. K. Chaudhary, "Analysis of a wideband circularly polarized cylindrical dielectric resonator antenna with broadside radiation coupled with simple microstrip feeding," *IEEE Access*, vol. 5, pp. 19478–19485, 2017.

[3] W.-J. Sun, W.-W. Yang, P. Chu, and J.-X. Chen, "Design of a wideband circularly polarized stacked dielectric resonator antenna," *IEEE Trans. Antennas Propag.*, vol. 67, no. 1, pp. 591–595, Jan. 2019. doi: 10.1109/TAP.2018.2874678.

[4] X. Cui, F. Yang, and M. Gao, "Wideband CP magnetoelectric dipole antenna with microstrip line aperture-coupled excitation," *Electron. Lett.*, vol. 54, no. 14, pp. 863–864, Jul. 2018.

[5] M. Qu, L. Deng, M. Li, L. Yao, and S. Li, "Compact sequential feeding network with quadruple output ports and its application for wideband circularly polarized antenna," *IEEE Access*, vol. 6, pp. 31891–31898, Apr. 2018.

[6] X. Chen, L. Wang, D. Wu, J. Lei, and G. Fu, "Compact and wideband directional circularly polarized distributed patch antenna with high efficiency," *IEEE Access*, vol. 5, pp. 15942–15947, Aug. 2017.

[7] R. Xu, J.-Y. Li, and J. Liu, "A design of broadband circularly polarized c-shaped slot antenna with sword-shaped radiator and its array for L/S-band applications," *IEEE Access*, vol. 6, pp. 5891–5896, Dec. 2017.

[8] H.-D. Chen, "Broadband CPW-fed square slot antennas with a widened tuning stub," *IEEE Trans. Antennas Propag.*, vol. 51, no. 8, pp. 1982–1986, Aug. 2003.

[9] R. Xu, J. Li, J. Liu, S. G. Zhou, and K. Wei, "UWB circularly polarised slot antenna with modified ground plane and L-shaped radiator," *Electron. Lett.*, vol. 54, no. 15, pp. 918–920, Jun. 2008.

[10] M. Midya, S. Bhattacharjee, and M. Mitra, "Pair of grounded L strips loaded broadband circularly polarised square slot antenna with enhanced axial ratio bandwidth," *Electron. Lett.*, vol. 54, no. 15, pp. 917–918, Jul. 2008.

[11] J. W. Baik, K. J. Lee, W. S. Yoon, T. H. Lee, and Y. S. Kim, "Circularly polarised printed crossed dipole antennas with broadband axial ratio," *Electron. Lett.*, vol. 44, no. 13, pp. 785–786, Jun. 2008.

[12] T. K. Nguyen, H. H. Tran, and N. N. Tong, "A wideband dual-cavity-backed circularly polarized crossed dipole antenna," *IEEE Antennas Wireless Propag. Lett.*, vol. 16, pp. 3135–3138, Oct. 2017.

[13] Y. He, W. He, and H. Wong, "A wideband circularly polarized cross-dipole antenna," *IEEE Antennas Wireless Propag. Lett.*, vol. 13, pp. 67–70, Jan. 2014.

[14] J.-W. Baik, T.-H. Lee, S. Pyo, S.-M. Han, J. Jeong, and Y.-S. Kim, "Broadband circularly polarized crossed dipole with parasitic loop resonators and its arrays," *IEEE Trans. Antennas Propag.*, vol. 59, no. 1, pp. 80–88, Jan. 2011.

[15] H. H. Tran and I. Park, "Wideband circularly polarized cavity-backed asymmetric crossed bowtie dipole antenna," *IEEE Antennas Wireless Propag. Lett.*, vol. 15, pp. 358–361, 2016.

[16] G. Feng, L. Chen, X. Xue, and X. Shi, "Broadband circularly polarized crossed-dipole antenna with a single asymmetrical cross-loop," *IEEE Antennas Wireless Propag. Lett.*, vol. 16, pp. 3184–3187, Oct. 2017.

[17] H. H. Tran, I. Park, and T. K. Nguyen, "Circularly polarized bandwidth-enhanced crossed dipole antenna with a simple single parasitic element," *IEEE Antennas Wireless Propag. Lett.*, vol. 16, pp. 1776–1779, 2017.

[18] Y. M. Pan, W. J. Yang, S. Y. Zheng, and P. F. Hu, "Design of wideband circularly polarized antenna using coupled rotated vertical metallic plates," *IEEE Trans. Antennas Propag.*, vol. 66, no. 1, pp. 42–49, Jan. 2018.

[19] L. Zhang, S. Gao, Q. Luo, P. R. Young, Q. Li, Y.-L. Geng, and R. A. Abd-Alhameed, "Single-feed ultra-wideband circularly polarized antenna with enhanced front-to-back ratio," *IEEE Trans. Antennas Propag.*, vol. 64, no. 1, pp. 355–360, Jan. 2016.

[20] L. Zhang and B. Sun, "Wideband circularly polarized crossed dipole antenna with parasitic elements," in *Proc. Cross Strait Quad-Regional Radio Sci. Wireless Technol. Conf. (CSQRWC)*, Jul. 2018, pp. 1–2.

[21] G. Feng, L. Chen, X. Wang, X. Xue, and X. Shi, "Broadband circularly polarized crossed bowtie dipole antenna loaded with parasitic elements," *IEEE Antennas Wireless Propag. Lett.*, vol. 17, no. 1, pp. 114–117, Jan. 2018.

[22] L. Wang, W.-X. Fang, Y.-F. En, Y. Huang, W.-H. Shao, and B. Yao, "Wideband circularly polarized cross-dipole antenna with parasitic elements," *IEEE Access*, vol. 7, pp. 35097–35102, 2019.

ZHIPENG ZHAO received the B.S. degree from Xidian University, Xi'an, China, in 2015, where he is currently pursuing the Ph.D. degree in electromagnetic field and microwave technology from the National Key Laboratory of Antennas and Microwave Technology.

His research interests include circular polarized antenna, wideband antenna, series-fed microstrip antenna array, and filtering antenna.

YAPENG LI received the B.S. degree from Xidian University in 2012 and the M.S. degree from Lanzhou Jiaotong University in 2016. He is currently pursuing the Ph.D. degree in electromagnetic field and microwave technology from the National Key Laboratory of Antennas and Microwave Technology, Xidian University, Xi'an, China. His research interests include filtering antenna, wideband antenna, and circular polarized antenna.

MENG XUE received the B.S. degree from the Nanjing University of Posts and Telecommunications in 2016. He is currently pursuing the M.S degree in electromagnetic field and microwave technology from the National Key Laboratory of Antennas and Microwave Technology, Xidian University, Xi'an, China. His research interests include dual-polarized antenna and wideband antenna.

LE WANG received the B.S. degree from Xidian University, Xi'an, China, in 2016, where he is currently pursuing the master's degree in electromagnetic field and microwave technology from the National Key Laboratory of Antennas and Microwave Technology. His research interests include series-fed antenna array, partial reflective surface, and impedance match.

ZHAOYANG TANG received the B.S. and M.S. degrees from Xidian University, Xi'an, China, in 2013 and 2016, respectively, where he is currently pursuing the Ph.D. degree in electromagnetic field and microwave technology from the National Key Laboratory of Antennas and Microwave Technology. His research interests include multiband antennas, ultra-wideband antennas, and antennas for base stations.

YINGZENG YIN received the B.S., M.S., and Ph.D. degrees in electromagnetic wave and microwave technology from Xidian University, Xi'an, China, in 1987, 1990, and 2002, respectively.

From 1990 to 1992, he was a Research Assistant and an Instructor with the Institute of Antennas and Electromagnetic Scattering, Xidian University, where he was an Associate Professor with the Department of Electromagnetic Engineering from 1992 to 1996, and has been a Professor since 2004. His current research interests include the design of microstrip antennas, feeds for parabolic reflectors, artificial magnetic conductors, phased array antennas, base-station antennas, and computer aided design for antennas.